PCCP

Accepted Manuscript




ROYAL SOCIETY OF CHEMISTRY

www.rsc.org/pccp

# First principles study on stability and hydrogen adsorption properties of Mg/Ti interface

J. H. Dai, R.W. Xie, Y. Y. Chen, and Y. Song*

*School of Materials Science and Engineering, Harbin Institute of Technology at Weihai, 2 West Wenhua Road, Weihai 264209, China*

**Abstract**

The hydrogenation and stability properties of Mg/Ti interface are studied by first-principles calculations. The strain of lattice and movement of ions were imposed to search the stable Mg/Ti interface. The anti-symmetrical configuration was found to be the most stable. The easiest transition pathway from anti-symmetrical to symmetrical configuration may be through the diagonal direction with no energy barrier. The hydrogen adsorption at distinguished positions in Mg/Ti interface is investigated. The negative hydrogen adsorption energy reaches -0.991 eV at the top site in the interface, which will highly favor the thermodynamic stability of Mg/Ti interface. The electronic structure is studied and found the Ti acts as a hydrogen atom 'capturer' and strong interactions between H and its surrounding Ti and Mg atoms are expected. Thus, inserting of Ti layers could create an interfacial zone where the adsorptions of hydrogen atoms may get stabilized and therefore improve the hydrogen storage properties of Mg.

Keywords: Mg/Ti interface; first principles; stability; capacity; hydrogenation

## 1. Introduction

Hydrogen energy is a promising energy carrier owing to the sustainable and clean characteristics. One of the key challenges using hydrogen practically is to store it in proper media. Hydrogen storage in metal hydride provides high safety but usually poor thermodynamics and kinetics. Efforts have been performed to design a storage medium with high hydrogen storage capacity, low cost, and proper thermodynamics and kinetics. $MgH_2$ has

* Corresponding author's email address: sy@hitwh.edu.cn

been extensively studied due to its high hydrogen storage capacity and light weight. However, the high dehydrogenation temperature and slow hydrogen sorption kinetics limit its practical applications.[1-5] Generally, the $Mg+H_2 \rightarrow MgH_2$ reaction starts from the reaction of hydrogen with Mg(0001) surface.[6] Extensively studies have been performed on the adsorption and dissociation mechanisms of hydrogen molecule on Mg(0001) surface.[7-9] Alloying with Ti greatly improves the adsorption/dissociation of hydrogen on Mg(0001) surface,[10-13] in which the dissociation/recombination of $H_2$ is the rate-limiting step of the overall reaction.[14] Thin Ti inter-layers in Mg film can significantly improve the hydrogen sorption kinetics and reversibility, which offers an effective way to improve the hydrogen storage properties of thick Mg-based films.[15] The strong interactions between Ti and hydrogen atoms in $MgH_2$ bring the great distortions of $MgH_2$ phase and potentially generate the $TiH_2$ phase.[16]

To understand the role of Ti inter-layers on the hydrogen adsorption of Mg film, one should keep in mind that adsorption of hydrogen atoms on the surface of Mg and Ti shows different behaviors. Adsorption of hydrogen atoms shows negative adsorption energy on both Ti(0001) and Mg(0001) surfaces.[17-19] However, H atoms prefer to pair up to form clusters on Mg surface, while they tend to adsorb away as far as possible on Ti surface. This may originate from the different bonding characteristics of H in Mg and Ti hydrides, *i.e.*, the Mg-H bond in Mg hydride is more ionic than that of Ti-H bond in Ti hydride.[20] The dissociation barrier of hydrogen molecule on pure Mg(0001) surface is around 1.06 eV,[21,22] while it decreases to 0.103 eV on Ti-incorporated Mg(0001) surface due to the strong interactions between hydrogen and Ti.[11,22]

Previously, we have studied the hydrogenation behaviors of Mg/TiAl sandwiched films.[23] The Mg/TiAl sandwiched films are thermodynamically stable and the inserting of TiAl layers into Mg films greatly increases the hydrogen adsorption ability of Mg films. In the present work, the interface between Mg(0001) and Ti(0001) slabs and its hydrogenation behaviors are studied via first-principles calculations. The method used in this paper is briefly described in Section 2, and results are presented in Section 3. Electronic structures are analyzed to identify the intrinsic mechanisms of hydrogenation of Mg/Ti interface. Conclusions are presented in the last part.

## 2. Computation method

A (2×2) slab model with 7 atomic layers stacking along *c* direction and a 1.8 nm vacuum containing 28 Mg atoms are used to simulate the Mg(0001) slab. Mg/Ti layered interfaces are built up with a 7-layer Mg(0001) and a 8-layer Ti(0001) slabs. *Vienna Ab-initio Simulation Package* (VASP) is employed to perform all calculations.[24,25] The projector augmented wave (PAW) method to describe the characteristics of nuclei and core electrons and the generalized gradient approximation with the Perdew-Wang 91 (GGA-PW91) of exchange-correlation function[26,27] were used. A energy cutoff of 400 eV of plane wave basis set was used in all calculations. The calculations about following 'Stability of Mg(0001)/Ti(0001) interfaces' are carried out based on the (1×1) slab model with a 20×20×1 Monckhorst-Pack[28] k-point grid. The 'Adsorption of hydrogen' is calculated with a (2×2) slab model in order to avoid the interactions between hydrogen atoms. The 7×7×1 k-point grid was used for (2×2) slab based on the considerations of accuracy and consumption of computer. The detailed tests on the k-point grid and the energy cutoff are shown in Fig. S1 in Supporting Information. The convergence criteria of self-consistency calculations are that the differences between two consecutive energies and forces are less than 0.01 meV and 0.01 eV/Å, respectively. Relaxations of the coordinates of all atoms except the bottom layer are carried out.

## 3. Results and discussions

### 3.1. Stability of Mg(0001)/Ti(0001) interfaces

Both metals Mg and Ti are hexagonal closed packing structure at ground state. There are two possible stacking configurations between the Mg(0001) and Ti(0001) slabs. The AB...BA|AB...AB stacking (denoted as SA), and the AB...BA|BA...AB stacking (denoted as AA), where the Mg and Ti atoms are in symmetrical and anti-symmetrical positions to the Mg/Ti interface as shown in Figs. 1 (a) and (b), respectively. The lattice parameters are $a$ = 3.209 Å (Mg) and 2.951 Å (Ti), respectively. Therefore, a lattice misfit will occur when they construct the Mg(0001)/Ti(0001) interface. The treatment of the lattice misfit problem is highly misfit dependent. For small misfits, the over-layer is supposed to accept the substrate lattice parameters, while the supercell is constructed by using multiple unit cells of both

counterparts in an appropriate ratio for a system with a large misfit.[29] There is no available general approach to deal with the moderate misfits. The "*stress balancing*" approach, which takes into account linear elasticity in the most general description, was proposed for this problem recently.[30] In the present work the "stress balancing" approach was applied, *i. e.*, we applied strains on both sides. Choosing the average area of Mg(0001) and Ti(0001) surfaces as the reference, the ratio of the interface area over this average value is used as a parameter, so-called the scaling factor of interface, to describe the strains applied. The influence of the separation, $d$, between the Mg and Ti slabs and the scaling factor of interface was examined by calculating formation energy ($E_f$) of the AA and SA models on the two parameters. The formation energy is defined as:

$$E_f = E_{inter} - E_{\text{Mg slab}} - E_{\text{Ti slab}} \quad (1)$$

where $E_{inter}$ is the total energy of Mg/Ti interface. $E_{\text{Mg slab}}$ and $E_{\text{Ti slab}}$ are the total energies of Ti(0001) and Mg(0001) surfaces with same configurations in Mg/Ti interface. Results are shown in Fig. 2. The minimum values of -0.856 eV and -0.523 eV appear at 0.991 scaling factor of interface and 2.4 Å separation for the AA interface (Fig. 2(a)) and at 0.979 scaling factor of interface and 3.0 Å separation for the SA interface (Fig. 2(b)). The sizes of the relaxed AA and SA interface supercells are $a = b = 3.049$ Å and 3.018 Å, and $c = 51.4$ Å, respectively.

It can be noted that the two configurations have similar stability, the AA model is slightly more stable than the SA model (only 0.33 eV energy difference). The transition between the SA and the AA stacking can be achieved by moving one part of the interface model straightforwardly along the dash line in Fig. 1(c), or alternatively alone the solid line step by step, relative to the other part. To estimate the energy barrier of this transition, an energy surface was calculated by changing the positions of atoms along the solid lines in Fig. 1(c) with a 11×11 mesh. All calculations are performed with fixed lattice parameters corresponding to the minimum energy points in Figs. 2(a) and (b). Results are shown in Fig. 3. It should be noted that the length of the edges in Fig. 3(a) is one over three of the size of the interface. The highest energy zone appears in the SA corner and along the $b'$ direction, while the lowest energy zones mainly occur around the AA corner. To estimate the transition barrier

between SA and AA models, three possible transition pathways, SA-a-b-AA, SA-b′-a′-AA, and SA-c-AA, were examined. Fig. 3(b) illustrates the calculated results. It shows that the easiest pathway from the SA to AA is the SA-c-AA, in which the energy gradually decreases without barrier, following by the SA-a-b-AA with a barrier of 0.71 J/m$^2$. The barrier of the transition from SA-b′-a′-AA pathway has to undergo mounts of high energy zone.

The similar stability between the AA and SA configurations originates from the electronic distribution in/around the interface. The difference of the plane-averaged charges (PACs) between the interface system and the individual Mg and Ti slabs was analyzed and shown in Fig. 4. It shows that redistribution of electrons occurs in/around the interface (mainly within two atomic layers in both sides). A relatively large amount of electrons donated from the most front layers of both Mg and Ti was accumulated in the interface zone. This makes a covalent bond between Mg and Ti atoms and potentially provides attracting source for hydrogen when it is used as a hydrogen storage medium. Inside the slabs the charge redistributions in Mg and Ti slabs illustrate opposite characteristics: charge redistribution extends deeper in Mg slab than that in Ti slab; Ti sublayer collects electrons while Mg sublayer loses electrons; and the interlamination near the interface becomes a rich-electron zone in Mg side but a poor-electron zone in Ti side.

### 3.2 Adsorption of hydrogen

Formation of the Mg/Ti interface creates a distortion zone around the interface, which can be divided into two areas, the separation area and the subsurface layers. The adsorption sites of hydrogen atom in the separation area were selected at bridge, fcc, hcp, and top sites referring to the Mg slab as shown in Fig. 5(a). The detailed adsorption sites of hydrogen in the interface model are shown in Table S1 in Supporting Information. For the subsurface layer adsorption, two tetrahedral sites and one octahedral site in both Mg and Ti slabs are considered and illustrated in Fig. 5(b). The adsorption energy of hydrogen is evaluated via the following definition:

$$E_{ads} = E_{\text{inter+H}} - E_{\text{inter}} - \mu_{\text{H}} \quad (2)$$

Here, $E_{\text{inter+H}}$ and $E_{\text{inter}}$ denote the total energies of the Mg/Ti interfaces with and without H

atom. The $\mu_H$ is the chemical potential of a hydrogen atom. In the present work the chemical potential of hydrogen atom is considered as the half of total energy of the hydrogen molecule in gas phase. The calculated adsorption energy of one hydrogen atom in Mg/Ti interface is listed in Table 1. All considered sites show negative adsorption energies indicating the hydrogenation properties of Mg slabs are greatly improved by inserting of Ti slabs. The top site, with negative absorption energy of -0.991 eV wins the most stable adsorption site. Comparing to the bulk and the surface adsorption of hydrogen in Mg, Mg/Ti interface creates more stable circumstance for hydrogen to be adsorbed. Table 1 also shows that hydrogen atoms tend to be adsorbed in the subsurface of Ti rather than the subsurface of Mg.

In order to compare the hydrogen adsorption preference quantitatively, we calculated the charge difference referring to the isolated H atom in a sphere centered at the hydrogen atom. The difference of charge around the H atom is caused by the interactions with its vicinity of Mg or Ti atoms. The numbers of charge difference in a sphere centered in the H atom are integrated by summing up the charge difference between self-consistent and non-self-consistent charge of Mg/Ti interface. Fig. 6 shows the value of charge difference *vs* sphere radius of the H atom. For all cases the charge monotonously increases with the radius of the sphere until to 0.9 Å, meaning the hydrogen atom is ionized by the adsorption. The ionization is strong when H adsorbs in Mg slab and weak in Ti slab. The bonding of H atom with Mg atoms is highly ionic while it shows a mixture of covalent and ionic interaction between H and Ti atoms, which are consistent with the bonding characteristics of H in Mg and Ti hydrides. In the separation zone, the two stable adsorption sites, the top and the fcc sites, appear a maximum charge accumulation of 0.7 *e* meaning a covalent bond between H and metal atoms is expectable.

**3.3 Electronic structures**

Fig. 7 shows partial density of states (PDOS) of atoms in Mg/Ti interface. Labels Mg3 and Ti3 indicate the atoms in the interface region, Mg2 and Ti2 state the atoms in bulk region, and Mg1 and Ti1 are the atoms in the surface layers. The bonding peaks of Mg atoms mainly distributed in the energy region of (-5.0, -4.0) eV, dedicating the bonding between Mg atoms. The Ti-Ti bonding interactions mainly occur in the energy region from -2.0 eV to the Fermi

energy level. All valence orbitals of Mg and Ti across the Fermi energy level showing explicitly metallic characteristics. The PDOS of Mg2 illustrates the bonding characteristics between bulk Mg atoms. The DOS of Mg3 (in the interface zone) is larger than those of Mg2 (in the bulk) in the energy range from -0.5 eV to the Fermi energy level, which indicates a high activity of the Mg3 than the Mg2 atoms. Similar characteristics are also observed from the Ti side. This could benefit the adsorption of H atoms in the interface zone. The *s* orbital of surface Mg1 atom shows relatively high activity. In the fourth panel of Fig. 7(a), Ti3 *d* orbital appears two bonding peaks in energy region of -0.5 eV to the Fermi energy level, and overlaps well with Mg3 *s* and *p* orbitals. This contributes to the Mg-Ti bonding. There are sharp peaks of both Mg and Ti atoms around -2.0 eV, and the amplitudes of peaks are gradually decreased from Mg1(Ti1) to Mg3(Ti3) atoms. Therefore, the formation of Mg/Ti interface is associated by the transition of surface states of Mg and Ti atoms to the bonding region of -0.5 eV to the Fermi energy level, which enhances the bonding interactions between Ti and Mg slabs, as illustrated in the PACs in Fig. 3.

The electron localization function (ELF)[31,32] is further calculated to study the transfers of electrons and the interaction between Mg and Ti slabs. The ELF is highly connected with the electron localization: ELF = 1 and 0 means the perfect localization of electron and no electrons in there, respectively. The distributions of ELF in the interfacial zone of Mg/Ti interface are shown in the Fig. 8 with scale from 0.8 (red) to 0.0 (blue), in which the bridge (bri), fcc, hcp and top sites are labeled. The distributions of ELF are highly symmetrical. The red regions are distributed around the top site (relative to Mg atoms), and the blue parts denotes the hcp site. The value of ELF decreases in the order of top, fcc, bri, and hcp sites. Due to the electrons mainly transfer from Ti to Mg atoms, the Mg may become more helpful for the adsorption of hydrogen atoms.

The PDOS of hydrogen atoms adsorbed at different sites is plotted in Fig. 9. The bonding peaks of hydrogen atoms mainly distributed around -7.0 eV. The bonding peaks of hydrogen in Ti environment are more concentrated than in Mg environment, which means there are stronger bonding interactions between H and Ti than H and Mg. It is well coincident with above analysis of charge difference and adsorption energy.

It is the most stable configuration that the hydrogen atom is adsorbed at the top site in

the Mg/Ti interface. The PDOSs of this hydrogenated Mg/Ti interface are shown in Fig. 10. It shows that the H-Mg(Ti) bonding occurs by the *s* orbital overlaps around -6.7 eV. Ti1, Ti2, and Ti3 atoms appear high similarity in the PDOSs with much higher amplitude than the PDOSs of Mg1. Therefore the Ti *d* orbital, which donates electron to the H *s* orbital, is the main attraction force for H atom. Other adsorption sites show similar bonding characteristics with this site. Therefore, it could be expected that Ti performs stronger attraction to hydrogen atoms, in which it improves the hydrogen adsorption properties of pure Mg.

## 4. Conclusions

In summary, first-principles calculations are performed to study the stability and hydrogen adsorption properties of Mg/Ti interface. The stabilities and configurations of the interface systems are investigated. The AA interface with 2.4 Å separation between Ti and Mg slabs with 0.991 scaling factor owns the most stability. The hydrogen adsorption properties and the interaction mechanisms of Mg/Ti interface are further investigated. Hydrogen adsorption energy at all considered sites appears negative values. The hydrogen prefers to adsorb in Ti environment. Electronic structures are analyzed to study the bonding characteristics in Mg/Ti interface and explore the hydrogen adsorption mechanisms. The bonding peaks of hydrogen in Ti environment are more concentrated than in Mg environment, and appear a covalent bond between H and metal atoms in top and fcc sites. Therefore, inserting of Ti layers could create an interfacial zone, where it can be activated to possess stronger ability to capture hydrogen atoms and further improves the hydrogenation properties of Mg.

## Acknowledgments

This work was supported by the National Basic Research Program of China, Grant No. 2011CB606400-G, the Natural Science Foundation of Shandong, China, Grant No. ZR2014EMM013, the Natural Science Foundation of Shandong, China, Grant No. ZR2014EMQ009, and the Fundamental Research Funds for the Central Universities Grant No. HIT.KITP.2014030. Simulations were performed using HPC resources in CAS Shenyang Supercomputing Center.

**References**


1 J. Olsen J Q.gy 1 B. Bogdanović, Th. Hartwig, B. Spliethoff, *Int J Hydrogen Energy*, 1993, **18**, 575-589.

2 L. Schlapbach, A. Zuttel, Nature, 2001, **414**, 353-358.

3 B. Sakintuna, F. Lamari-Dark rim, M. Hirscher, *Int J Hydrogen Energy*, 2007, **32**, 1121-1140.

4 A. Zaluska, L. Zaluski, J. Q. Ströme Olsen, *J Alloys Compd*, 1999, **288**, 217-225.

5 F. Y. Cheng, Z. L. Tao, J. Liang, *J. Chen, Chem Commun*, 2012, **48**, 7334-7343.

6 T. Jiang, L. X. Sun, W. X. Li, *Phys Rev B*, 2010, **81**, 035416-9.

7 M. Pozzo, D. Alfè, *J Phys Condens Matter*, 2009, **21**, 095004-4.

8 D. Kecik, M. K. Aydinol, *Surf Sci*, 2009, **603**, 304-310.

9 Y. F. Li, P. Zhang, B. Sun, Y. Yang, Y. H. Wei, *J Chem Phys*, 2009, **131**, 034706-10.

10 M. Pozzo, D. Alfè, A. Amieiro, S. French, A. Pratt, *J Chem Phys*, 2008, **128**, 094703-11.

11 M. Pozzo, D. Alfè, *Int J Hydrogen Energy*, 2009, **34**, 1922-1930.

12 A. J. Du, S. C. Smith, X. D. Yao, G. Q. Lu, *J Phys Chem B*, 2006, **110**, 21747-21750.

13 A. J. Du, C. Smith Sean, X. D. Yao, G. Q. Lu, *J Phys Chem B*, 2005, **109**, 18037-18041.

14 T. Vegge, *Phys Rev B*, 2004, **70**, 035412-7.

15 G. B. Xin, J. Z. Yang, H. Fu, W. Li, J. Zheng and X. G. Li, *RSC Advances*, 2013, **3**, 4167-4170.

16 J. H. Dai, Y. Song, R. Yang, *Int J Hydrogen Energy*, 2011, **36**, 12939-12949.

17 M. Wilde, K. Fukutani, *Phys Rev B*, 2008, **78**, 115411-10.

18 J. X. Guo, L. Guan, S. B. Wang, Q. X. Zhao, Y. L. Wang, B. T. Liu, *Appl Surf Sci*, 2008, **255**, 3164-3169.

19 G. X. Wu, J. Y. Zhang, Y. Q. Wu, Q. Li, K. C. Chou, X. H. Bao, *Acta Phys Chim Sin*, 2008, **24**, 55-60.

20 S. X. Tao, P. H. L. Notten, R. L. van Santen, A. P. J. Jansen, *Phys Rev B*, 2009, **79**, 144121-144127.

21 G. X. Wu, J. Y. Zhang, Y. Q. Wu, Q. Li, K. C. Chou, X. H. Bao, *Appl Surf Sci*, 2009, **255**, 6338-6344.

22 A. J. Du, S. C. Smith, X. D. Yao, G. Q. Lu, *J Phys Chem B*, 2005, **109**, 18037-18041.

23 J. H. Dai, Y. Song, B. Shi, R. Yang, *J Phys Chem C*, 2013, **117**, 25374-25380.

24 G. Kresse, J. Hafner, *Phys Rev B*, 1993, **47**, 558-561.

25 G. Kresse, J. Furthmüler, *Phys Rev B*, 1996, **54**, 11169-11186.

26 P. E. Blöchl, *Phys Rev B*, 1994, **50**, 17953-17979.

27 G. Kresse, J. Furthmüler, *Compt Mater Sci*, 1996, **6**, 15-50.

28 H. J. Monkhorst, J. D. Pack, *Phys Rev B*, 1976, **13**, 5188-5192.

29 S. Y. Liu, J. X. Shang, F. H. Wang, Y. Zhang, *Phys Rev B*, 2009, **79**, 075419.

30 W. H. Sun, G. Ceder, *Surf Sci*, 2013, **617**, 53-59.

31 A. D. Becke, K. E. Edgecombe,*J Chem Phys*, 1990, **92**, 5397-5403.

32 A. Savin, R. Nesper, S. Wengert, T. F. Fässler, *Angew Chem Int Ed Engl*, 1997, **36**, 1808-1832.

**Figures and Tables**

Fig. 1 − Supercells of Mg(0001)/Ti(0001) interface. (a) The side view of the SA (left) and the AA (right) couplings, and (b) the possible pathways of the transition between the AA and SA couplings. The brown and blue balls denote Mg and Ti atoms, respectively. The symbol *d* indicates the separation between Mg(0001) and Ti(0001) slabs.

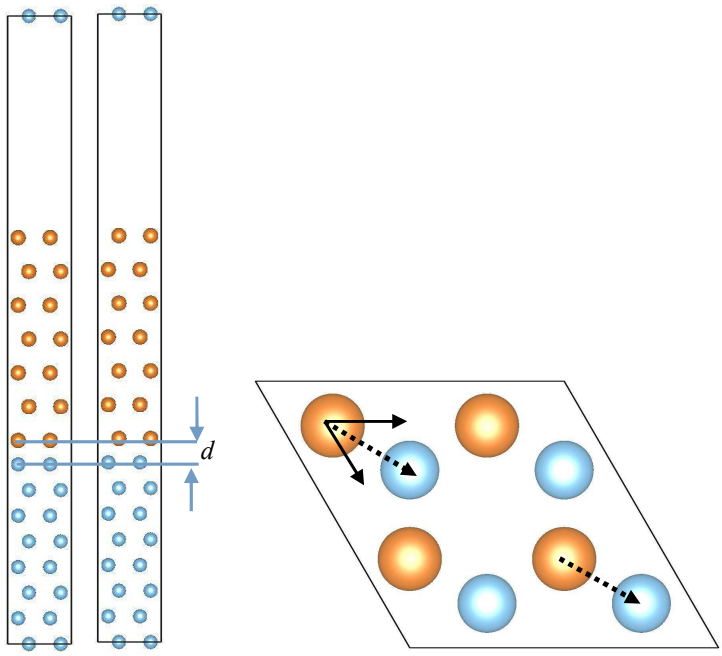

Fig. 2 − The variation of formation energies of interface against scaling factor and separation of interface. (a) AA and (b) SA systems.

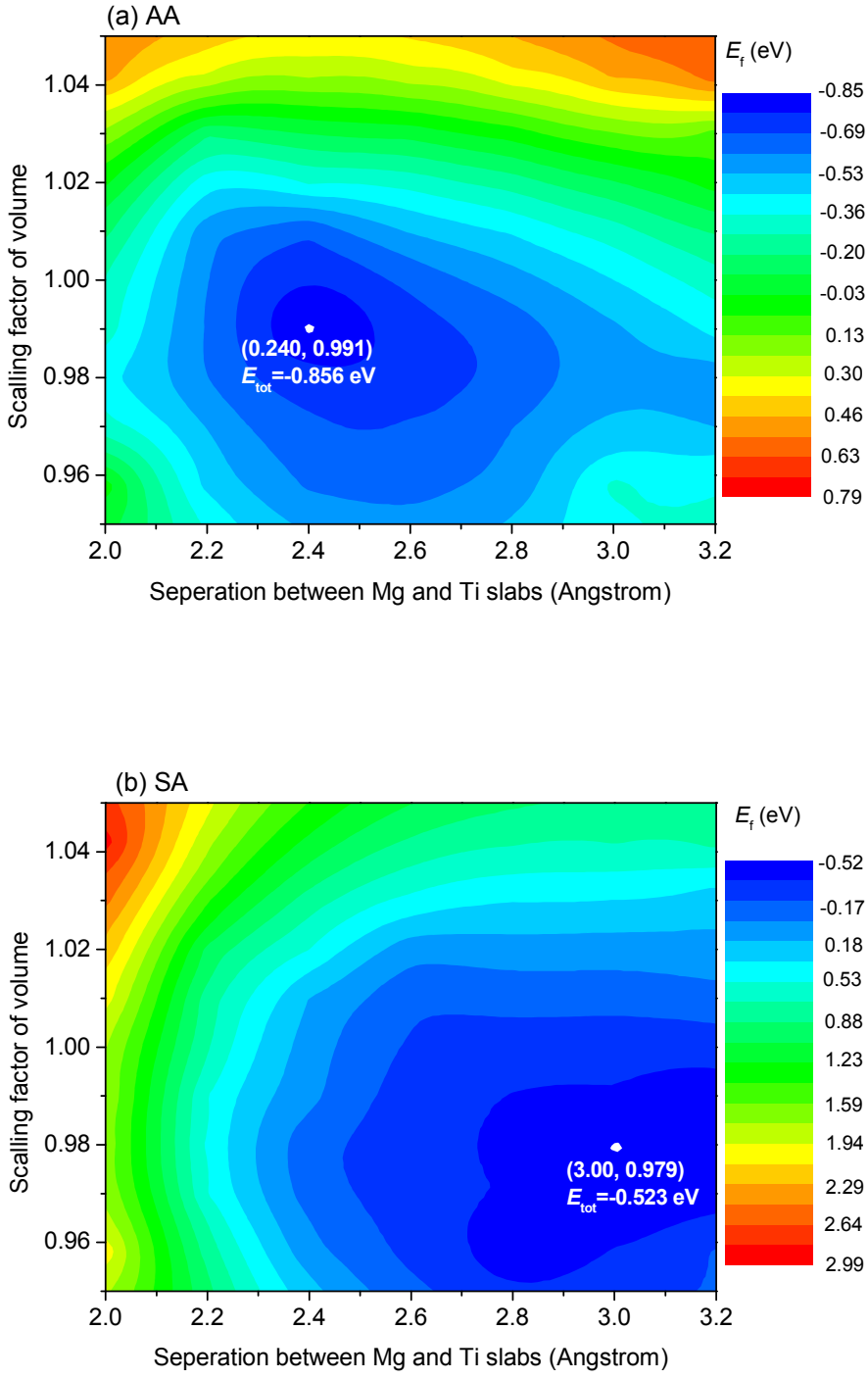

Fig. 3 – Energy of the interface against the relative shuffling between the Mg and Ti slabs. (a) energy surface and (b) alone special pathways.

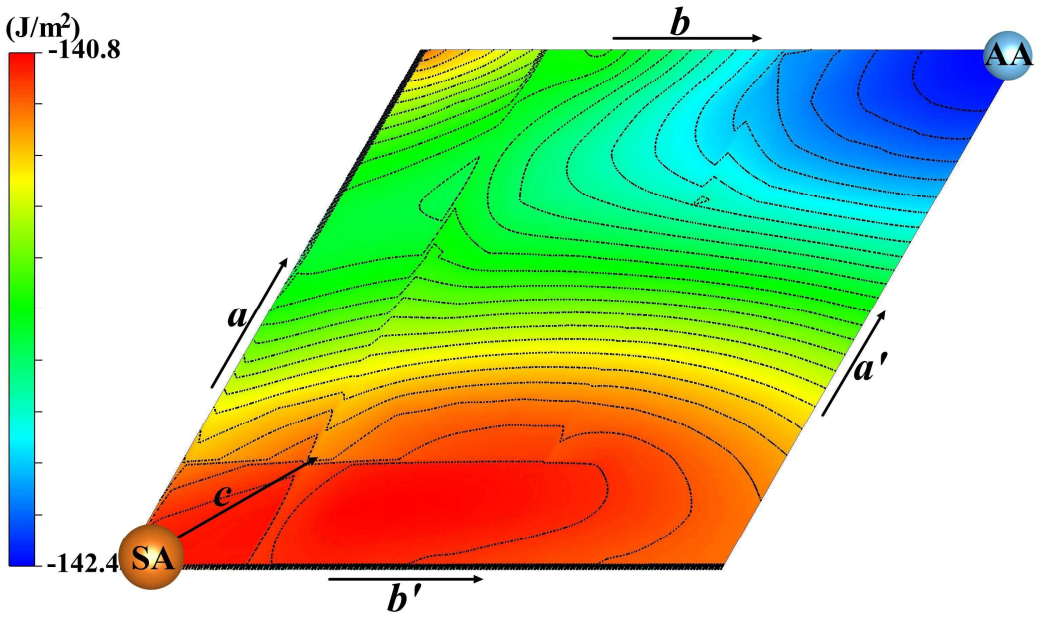


(a)

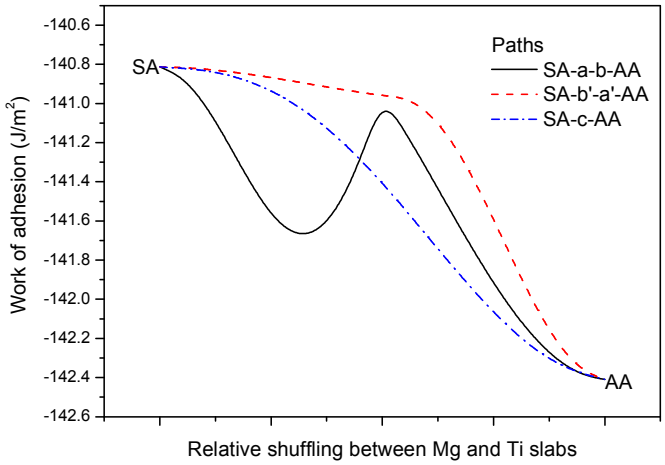


(b)

Fig. 4 – The difference of PACs of Mg/Ti interface.

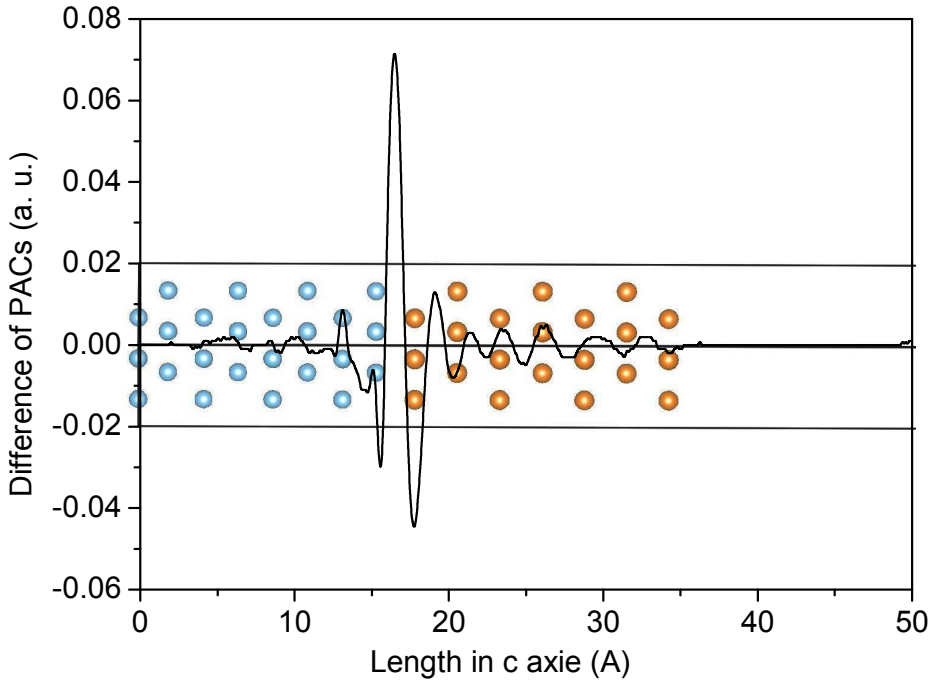


Fig. 5 − The occupation sites of hydrogen atom in Mg/Ti interface. The small pink and large brown balls denote H and metal atoms, respectively. (a) The top view of the occupation sites in the separation zone and (b) the side view of occupation sites under the most front layer.

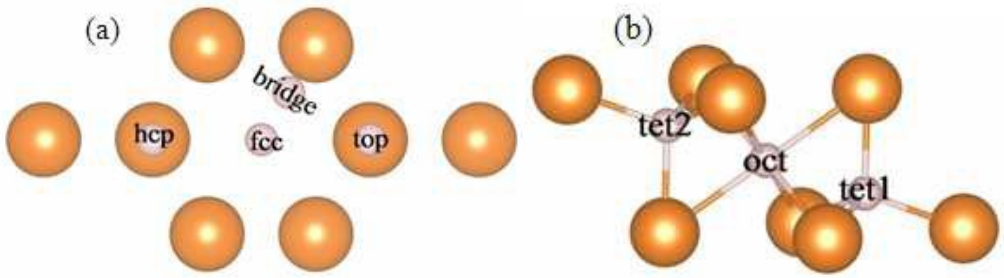

Fig. 6 – Value of charge difference *vs* sphere radius of the H atom.

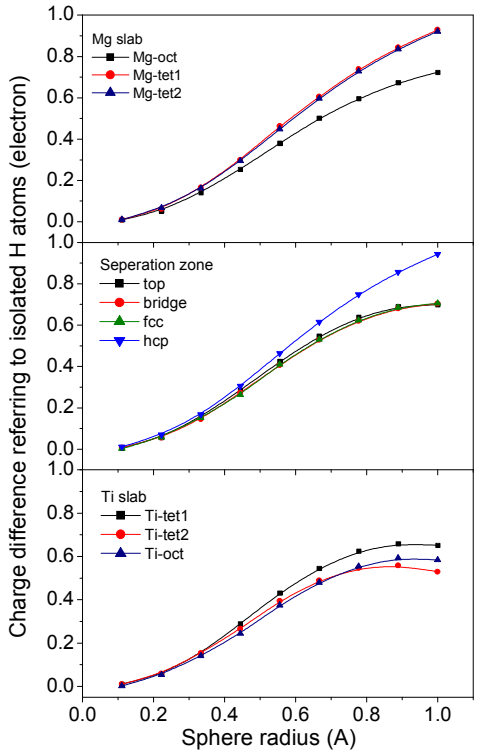


Fig. 7 − The total and partial densities of states of Ti and Mg atoms in Mg/Ti interface (a), where labels Ti1 to Mg3 are illustrated in (b).

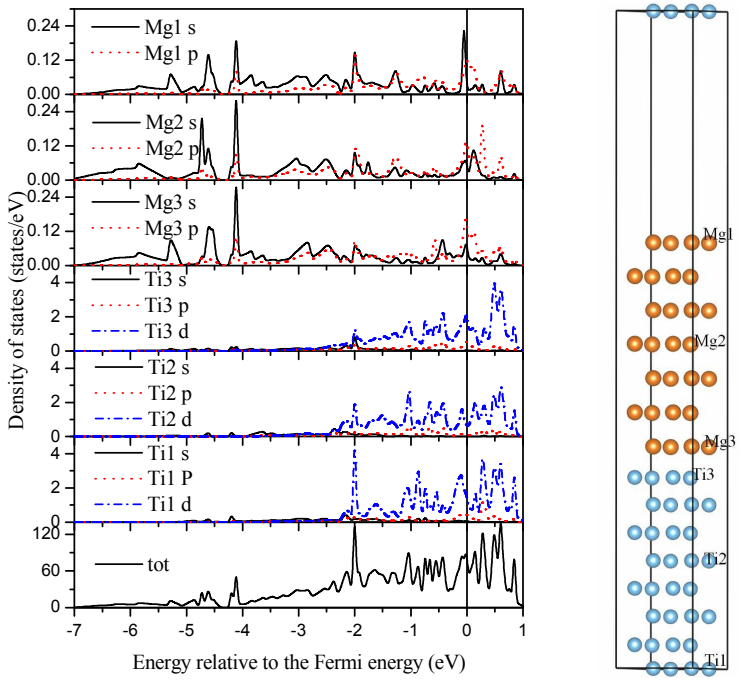


(a) (b)

Fig. 8 − The distribution of ELF in the interfacial zone of Mg/Ti interface.

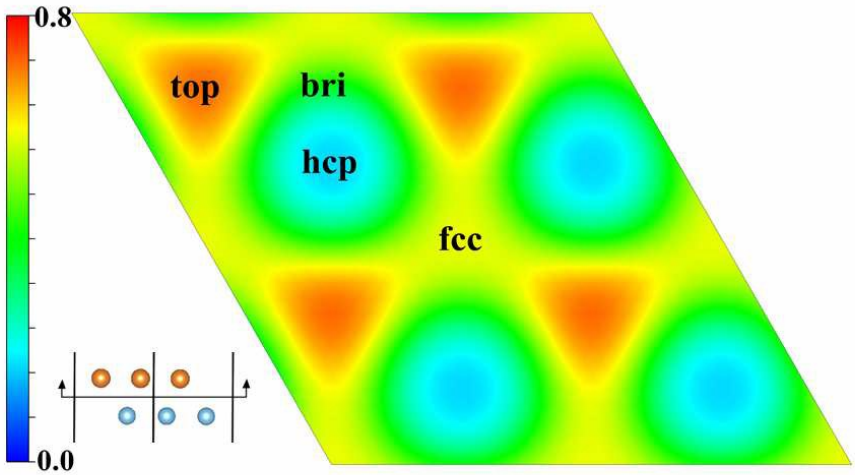

Fig. 9 − The density of states of hydrogen atoms in different positions.

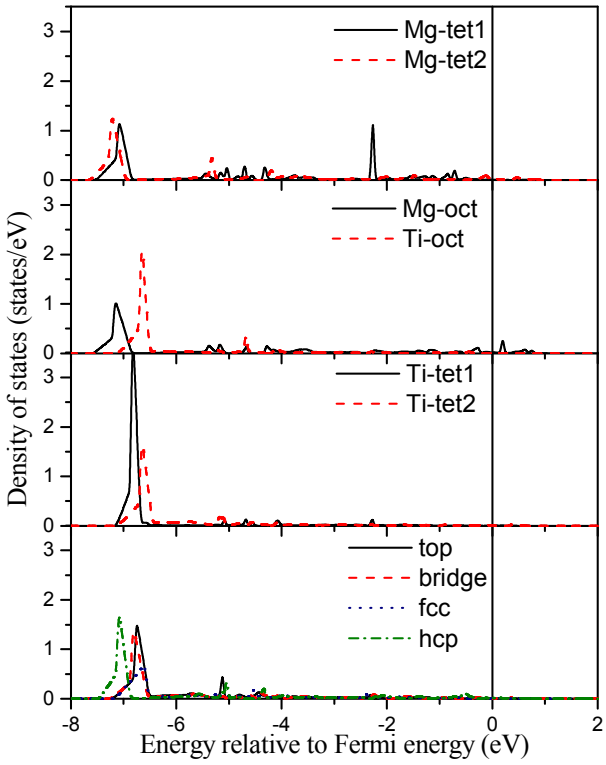

Fig. 10 − The total and partial densities of states of Mg/Ti interface with a hydrogen atom adsorbed at the top site in the Ti side (a), where H and its nearest neighbouring Mg, Ti1 and Ti2 atoms are illustrated in (b).

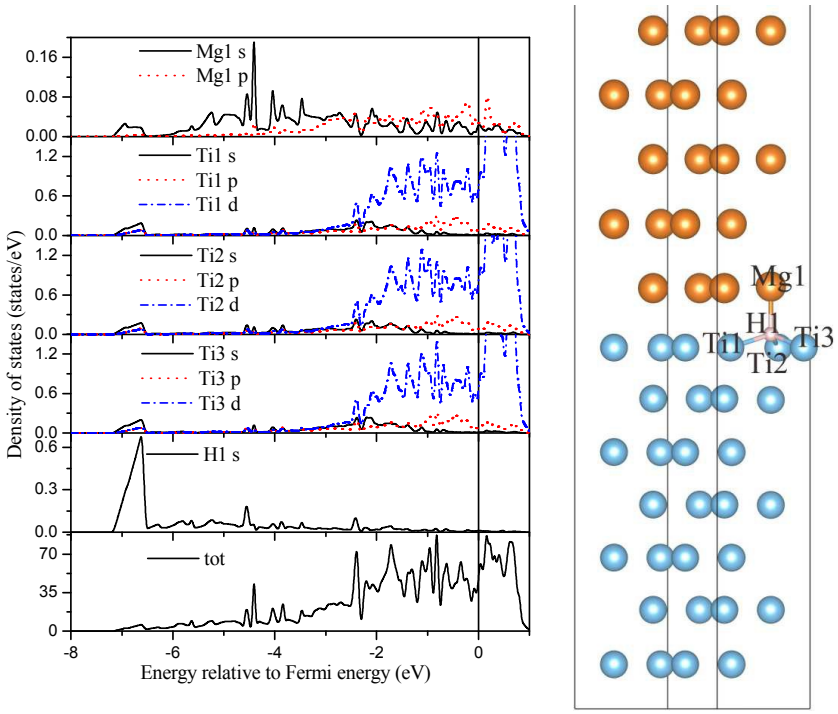


(a) (b)

Table 1 − The hydrogen adsorption energy (eV) in the Mg/Ti interface at different sites.

| H positions (interface) | $E_{ads}$ | H positions (sub-surfaces) | $E_{ads}$ |
|---|---|---|---|
| bridge | -0.932 | Mg-tet1 | -0.409 |
| fcc | -0.953 | Mg-tet2 | -0.141 |
| hcp | -0.408 | Mg-oct | -0.134 |
| top | -0.991 | Ti-tet1 | -0.783 |
| | | Ti-tet2 | -0.985 |
| | | Ti-oct | -0.961 |